

Structural, Elastic, Electronic and Optical Properties of a New Layered-Ternary Ta₄SiC₃ Compound

M. S. Islam and A.K.M.A. Islam *

Department of Physics, Rajshahi University, Rajshahi-6205, Bangladesh

ABSTRACT

We propose a new layered-ternary Ta₄SiC₃ with two different stacking sequences (α - and β -phases) of the metal atoms along c axis and study their structural stability. The mechanical, electronic and optical properties are then calculated and compared with those of other compounds M₄AX₃ (M = V, Nb, Ta; A = Al, Si and X = C). The predicted compound in the α -phase is found to possess higher hardness than any of these compounds. The independent elastic constants of the two phases are also evaluated and the results discussed. The electronic band structures for α - and β -Ta₄SiC₃ show metallic conductivity. Ta $5d$ electrons are mainly contributing to the total density of states (DOS). We see that the hybridization peak of Ta $5d$ and C $2p$ lies lower in energy and the Ta $5d$ -C $2p$ bond is stronger than Ta $5d$ -Si $3p$ bond. Further an analysis of the different optical properties shows the compound to possess improved behavior compared to similar types of compounds.

PACS: 60.20.Dc; 62.20.-x; 71.15.Mb; 78.20.Ci

Keywords: Ta₄SiC₃, First-principles; Elastic properties; Electronic properties; Optical properties.

1. Introduction

The layered-ternary compounds in the so-called MAX phases exist as M₂AX (211), M₃AX₂ (312) and M₄AX₃ (413) compounds, where M is an early transition metal, A is an A-group element (usually belonging to the groups IIIA and IVA) and X is either C or N. All these compounds show interesting properties, e.g. electrical and thermal conduction, high bulk modulus, high melting point, low density, low Vickers hardness, damage-tolerance, thermal shock resistance and so on, and have been investigated extensively [1-20].

Currently there are eight M₄AX₃ (413) compounds, such as Ti₄AlN₃, Ti₄SiC₃, Ti₄GeC₃, Ti₄GaC₃, Ta₄AlC₃, Nb₄AlC₃, V₄AlC₃, and V₄AlC_{2.69} which have been synthesized [9, 12-19]. Among these Ta₄AlC₃, a relatively new member of 413 phases was synthesized in the form of polycrystals [8-11] and single-crystals [12]. Subsequently two new 413 phases, Nb₄AlC₃ [16] and V₄AlC₃ [17] were synthesized and characterized. But Ta₄AlC₃ has drawn a lot of attention recently [8-13]. The bulk modulus of Ta₄AlC₃ is determined to be 261 GPa, which is so far the highest among all the MAX phases reported [7]. Further it has been found to possess high flexural strength, high fracture toughness with good electrical and thermal and improved mechanical properties [13].

The polymorphs of Ta₄AlC₃ have been identified by several workers [7, 10-12]. The two phases of Ta₄AlC₃ crystallize in a hexagonal structure with the space group $P6_3/mmc$ but have different atomic positions. One phase is α -Ta₄AlC₃, which is the same as Ti₄AlN₃, stacking sequence of the metal atom Ta and Al in the order of ABABACBCBC

* Corresponding author:

E-mail address: azi46@ru.ac.bd (A.K.M.A. Islam)

along c axis, reported by Etzkorn *et al.* [12]. The other phase, reported by Lin *et al.* [11, 20], is the so-called β - Ta_4AlC_3 which stacks in ABABABABAB along c axis.

As mentioned earlier Ta_4AlC_3 has excellent properties and it is envisaged that there may be other compounds that could be predicted with a different A-group element which could show more desirable properties. In order to explore new field of 413 phases we propose a new layered-ternary Ta_4SiC_3 and study its stability. Elastic properties are essential to the understanding of the macroscopic mechanical properties of crystals because they are related to various fundamental solid state properties and thermodynamic properties. A first-principles study of structural, elastic (for both mono- and polycrystalline aggregate) and electronic properties in the framework of density functional theory would be made. Further the optical properties (dielectric function, absorption spectrum, conductivity, energy-loss spectrum and reflectivity) will be calculated and discussed.

2. Computational methods

The first-principles *ab-initio* calculations are performed using the CASTEP code [21] in the framework of density functional theory (DFT) with generalized gradient approximation (GGA) and default the Perdew-Burke-Ernzerhof (PBE) [22]. The interactions between ion and electron are represented by ultrasoft Vanderbilt-type pseudopotentials for Ta, Si and C atoms [23]. The elastic constants are calculated by the ‘stress–strain’ method. All the calculating properties for Ta_4SiC_3 used a plane-wave cutoff energy 450 eV and $9 \times 9 \times 2$ Monkhorst-Pack [24] grid for the sampling of the Brillouin zone. Geometry optimization is conducted using convergence thresholds of 5×10^{-6} eV atom^{-1} for the total energy, 0.01 eV \AA^{-1} for the maximum force, 0.02 GPa for maximum stress and 5×10^{-4} \AA for maximum displacement.

3. Results and discussions

3.1 Structural properties

The proposed compound Ta_4SiC_3 is first assumed to have a crystal structure similar to Ta_4AlC_3 and also other M_4AX_3 compounds. We know that Ta_4AlC_3 possesses two types of structures, i.e. α - and β - forms with two different stacking sequences. We then perform

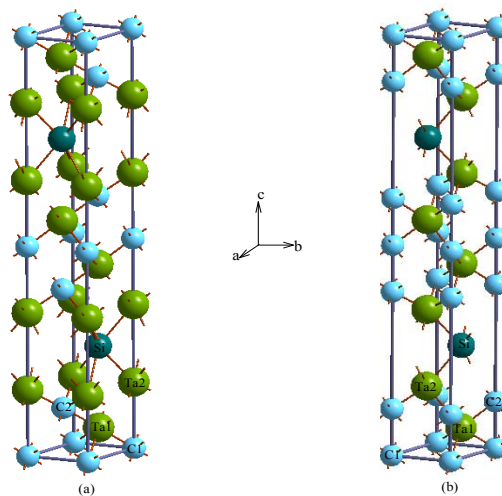


Fig. 1. Crystal structures of (a) α - Ta_4SiC_3 and (b) β - Ta_4SiC_3 .

the geometry optimization as a function of the normal stress by minimizing the total energy of the proposed compound for both these phases, i.e. α - and β -Ta₄SiC₃. The calculated total energy (-2247.77 eV) of α -Ta₄SiC₃ is more than that (-2246.74 eV) of β -Ta₄SiC₃, indicating α -Ta₄SiC₃ to be energetically more favourable. The crystal structures of α -Ta₄SiC₃ and β -Ta₄SiC₃ are illustrated in Fig. 1. The optimized parameters for both the phases are shown in (Table 1), along with those of other M₄AX₃, (M=V, Nb, Ta) compounds.

Table 1. The optimized structural parameters for both the structures of Ta₄SiC₃.

	a (Å)	c (Å)	c/a	V_0 (Å ³)	Ref.
α -Ta ₄ SiC ₃	3.2514	22.8900	7.04	209.60	This
β -Ta ₄ SiC ₃	3.1943	23.7290	7.43	209.70	This
α -Ta ₄ AlC ₃	3.134	24.268	7.74	206.42	[25] ^T
	3.138	24.163	7.70	206.05	[26] ^T
	3.312	24.111	7.75	229.04	[12] ^E
	3.109	24.708	7.74	206.82	[10] ^E
β -Ta ₄ AlC ₃	3.070	24.198	7.88	197.50	[27] ^T
	3.095	24.714	7.98	205.01	[26] ^T
	3.087	23.700	7.68	195.60	[7] ^E
	3.309	23.078	7.67	218.83	[27] ^E

T= Theoretical, E = Experimental.

3.2 Elastic constants and mechanical stability

To study the mechanical properties of α - and β -Ta₄SiC₃, we have calculated the elastic constants C_{ij} , bulk modulus B , shear modulus G , Young's modulus E , Poisson's ratio ν . The calculated results are illustrated in Table 2 along with other available theoretical results of several M₄AX₃ compounds. Both the structures have six elastic constants (C_{11} , C_{12} , C_{13} , C_{33} , C_{44} and C_{66}) and only five of them are independent, since $C_{66} = (C_{11} - C_{12})/2$. Both α - and β -Ta₄SiC₃ have C_{11} values smaller than those of α - and β -Ta₄AlC₃, which leads to the lower resistances against the principal strain ϵ_{11} . The C_{12} of α -Ta₄SiC₃ is 33 GPa larger than that of α -Ta₄AlC₃ and this leads to higher resistances against the principal strain ϵ_{12} . The C_{44} of α -Ta₄SiC₃ is 74 GPa larger than that of β -Ta₄SiC₃, thereby showing higher resistances to basal and prismatic shear deformations.

The criteria of mechanical stability are essential to illustrate a stable compound. The Born stability criteria [31] for α - and β -Ta₄SiC₃ are as follows:

$$\begin{aligned} C_{11} > 0, & \quad C_{11} - C_{12} > 0, \\ C_{44} > 0, & \quad (C_{11} + C_{12}) C_{33} - 2C_{13}^2 > 0. \end{aligned} \quad (1)$$

From the calculated elastic constants it is easy to see that these criteria are satisfied for both α -Ta₄SiC₃ and β -Ta₄SiC₃ and hence they are stable at zero pressure.

Table 2. Elastic constants C_{ij} , the bulk modulus B , shear modulus G , Young's modulus E (all in GPa), Poisson's ratio ν , anisotropic factor A , linear compressibility ratio k_c/k_a and ratio G/B at zero pressure.

	Monocrystal						Polycrystal						
	C_{11}	C_{12}	C_{13}	C_{33}	C_{44}	C_{66}	B	G	E	ν	A	k_c/k_a	G/B
α -Ta ₄ SiC ₃ ^a	396	190	180	391	207	103	254	138	350	0.27	2.00	1.07	0.54
β -Ta ₄ SiC ₃ ^a	397	148	190	397	133	124	250	121	312	0.29	1.06	0.80	0.48
α -Ta ₄ AlC ₃ ^b	454	157	156	376	201	149	247, 239 ^c	161	397	0.23			0.65
β -Ta ₄ AlC ₃ ^b	452	152	150	441	145	150	250, 240 ^c	148	370	0.25			0.59
α -Nb ₄ SiC ₃ ^c	403	167	165	374	195		241	142					0.59
α -Nb ₄ AlC ₃ ^c	413	124	135	328	161		214	144					0.67
V ₄ AlC ₃ ^d	458	107	110	396	175		218	170				1.21	0.78

^aThis work, ^bRef. [26], ^cRef. [36], ^dRef. [37], ^efitted value.

The theoretical polycrystalline elastic moduli for α - and β -Ta₄SiC₃ may be computed from the set of independent elastic constants. Hill's [28] proved that the Voigt and Reuss equations represent upper and lower limits of the true polycrystalline constants. According to Hill's observation, the polycrystalline moduli are defined as the average values of the Voigt (B_V , G_V) and Reuss (B_R , G_R) moduli. From Hill's observation, the value of bulk modulus (in GPa) $B = (B_V + B_R)/2 = B_H$ (Hill's bulk modulus), where B_V is the Voigt's bulk modulus and B_R is the Reuss's bulk modulus. The value of shear modulus (in GPa) $G = (G_V + G_R)/2 = G_H$ (Hill's shear modulus), where G_V is the Voigt's shear modulus and G_R is the Reuss's shear modulus. These expressions for Reuss and Voigt moduli can be found in ref. [29]. The polycrystalline Young's modulus E (in GPa) and the Poisson's ratio ν are then calculated using the relationships [30]: $E = 9BG/(3B + G)$ and $\nu = (3B - E)/6B$ respectively. The bulk modulus B of α -Ta₄SiC₃ is 7 GPa higher than that of α -Ta₄AlC₃. Table 2 shows that α -Ta₄SiC₃ possesses higher hardness due to its higher bulk modulus than the other M₄AX₃ compounds.

Using the calculated elastic constants C_{ij} , there are different ways to represent the elastic anisotropy of crystals. For this purpose, so-called shear anisotropy ratio $A = 2C_{44}/(C_{11} - C_{12})$ is often used [32]. The factor $A = 1$ represents complete isotropy, while values smaller or greater than this measure the degree of anisotropy. Therefore, α -Ta₄SiC₃ shows completely anisotropic behavior but β -Ta₄SiC₃ is nearly isotropic (Table 2).

The parameter $k_c/k_a = (C_{11} + C_{12} - 2C_{13})/(C_{33} - C_{13})$ is used, which expresses the ratio between linear compressibility coefficients of hexagonal crystals [33]. The data obtained $k_c/k_a = 1.07$ demonstrate that the compressibility for α -Ta₄SiC₃ along c axis is greater than along a axis and $k_c/k_a = 0.8$ that the compressibility for β -Ta₄SiC₃ along c axis is smaller than along a axis.

According to Pugh's criteria [34], a material should behave in a ductile manner, if $G/B < 0.5$, otherwise it should be brittle. For α -Ta₄SiC₃, $G/B = 0.54$, *i.e.* α -Ta₄SiC₃ is slightly above the borderline and for β -Ta₄SiC₃, $G/B = 0.48$, *i.e.* β -Ta₄SiC₃ will behave as a ductile material. For ductile metallic materials, Poisson's ratio ν is typically 0.33 [35], β -Ta₄SiC₃ shows greater ductility than that of α -Ta₄SiC₃.

The Debye temperature Θ_D is proportional to the average elastic wave velocity v_a . Then the Debye temperature Θ_D may be estimated from the average elastic wave velocity v_a [38]:

$$\Theta_D = \frac{h}{k_B} \left(\frac{3n}{4\pi V_0} \right)^{\frac{1}{3}} v_a \quad (2)$$

where h is Planck's constant, k_B is the Boltzmann's constant, V_0 is the volume of unit cell and n is the number of atoms in unit cell. Now the average elastic wave velocity v_a (m/sec) can be obtained from the transverse v_t and longitudinal wave velocity v_l , respectively (see [29]). Table 3 shows that α -Ta₄SiC₃ possesses larger elastic wave velocities and larger Debye temperatures Θ_D . The Debye temperatures for the predicted compounds in α - and β -phases are found to be lower than those of Ti₃SiC₂ (780 K), Ti₄AlN₃ (762 K) and Ti₃AlC₂ (758 K) [39].

Table 3. The transverse, longitudinal, average elastic wave velocities (v_t , v_l , v_a in m/sec) and Debye temperature (Θ_D in K) for α -Ta₄SiC₃ and β -Ta₄SiC₃.

Phase	ρ	v_t	v_l	v_a	Θ_D
α -Ta ₄ SiC ₃	12.48	3325	5924	4360	535
β -Ta ₄ SiC ₃	12.46	3116	5745	4092	502

3.3 Electronic properties

The energy band structures and DOS of α - and β -Ta₄SiC₃ are illustrated in Figs. 2 and 3. The valence and conduction bands overlap considerably and there are many bands crossing

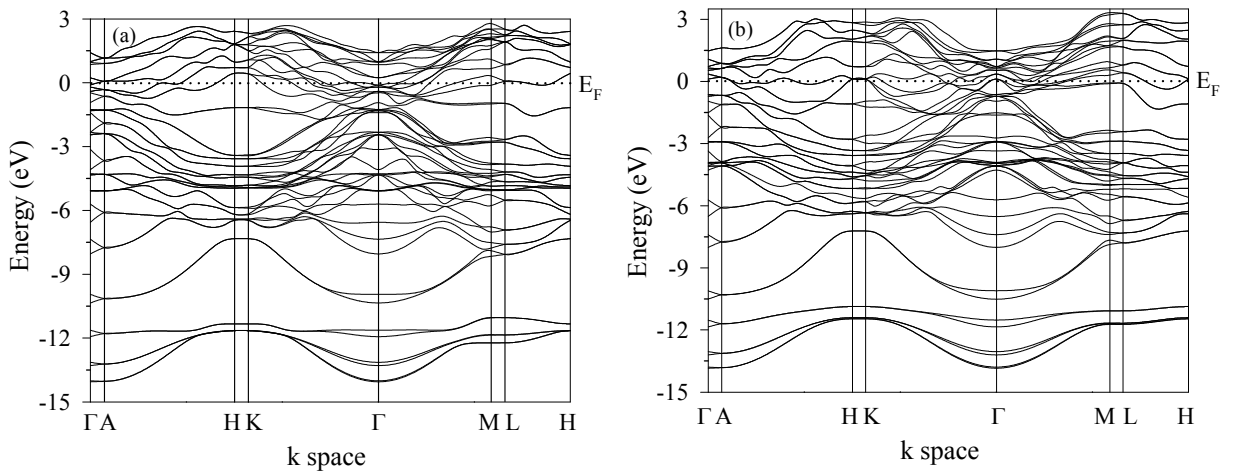


Fig. 2. Band structures of (a) α -Ta₄SiC₃ and (b) β -Ta₄SiC₃.

the Fermi level. Thus α - and β - Ta_4SiC_3 should show metallic conductivity. These energy bands around the Fermi energy are mainly from the Ta 5d states, suggesting that the Ta 5d states dominate the conductivity of Ta_4SiC_3 . It is apparent that Si 3s/3p electrons do not contribute significantly at the Fermi level for a scooping effect due to the presence of the Ta 5d states. The lowest valence bands from -14 to -10 eV below Fermi level ($E_F = 0$ eV) arise mainly from the C 2s states, with small contribution from the Ta 5d states. The higher valence bands between -8 and 0 eV are dominated by hybridizing Ta 5d, Si 3s/3p and C 2p states. Similar results are found with previous reports on M_4AX_3 phases [30, 36, 37]. As is evident the hybridization peak of Ta 5d and C 2p lies lower in energy than that of Ta 5d and Si 3p states. This suggests that the Ta 5d-C 2p bond is stronger than the Ta 5d-Si 3p bond.

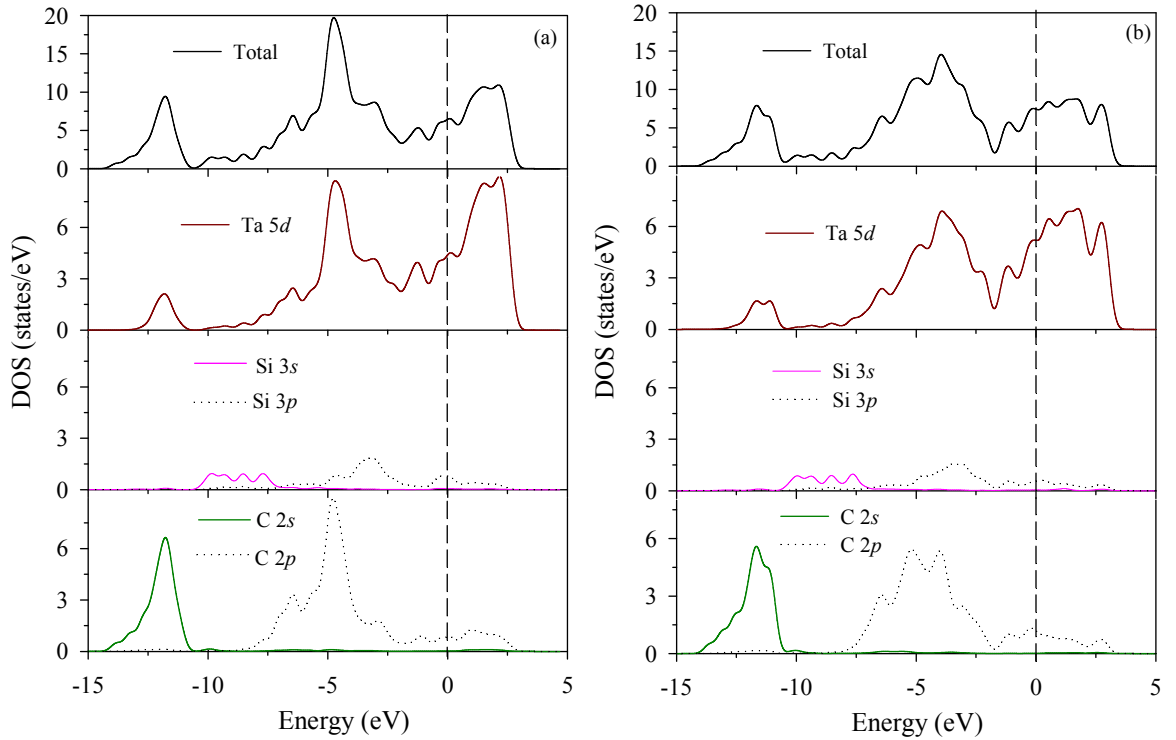


Fig. 3. Total and partial DOSs of (a) α - Ta_4SiC_3 and (b) β - Ta_4SiC_3 .

3.4 Optical properties

The optical constants of α - and β - Ta_4SiC_3 : real part and imaginary part of dielectric function $\epsilon_1(\omega)$ and $\epsilon_2(\omega)$, absorption, photoconductivity, energy-loss function, refractive index and reflectivity spectrum are shown in Figs. 4 and 5. We used a 0.5 eV Gaussian smearing for all calculations. For the imaginary part $\epsilon_2(\omega)$ of the dielectric function, the peak around 1 eV is due to transitions within the Ta 5d bands and the $\epsilon_2(\omega)$ spectrum above 5 eV arises from Si/C $p \rightarrow$ Ta d electronic transitions. The large negative value of $\epsilon_1(\omega)$ indicates that the Ta_4SiC_3 crystal has a Drude-like behavior.

In Fig. 4b, we show the absorption spectrum with one peak between 7.5 to 9 eV for α - Ta_4SiC_3 which rises and then decreases rapidly in the high-energy region. Nearly same feature can be seen for β - Ta_4SiC_3 but with two small peaks in the low energy side. The peak at around 7.4-8 eV is associated with the transition from Si/C p to Ta d states.

For both the structures, photoconductivity starts with zero photon energy. This shows that the material has no band gap. Moreover, the photoconductivity and hence electrical conductivity of a material increases as a result of absorbing photons [40]. The photoconductivity of α -Ta₄SiC₃ (Fig. 4c) shows three peaks at 1.8, 5.6, 14.4 (small) eV. β -Ta₄SiC₃ also shows peaks but at 1.14, 3.5, and 5.7 eV.

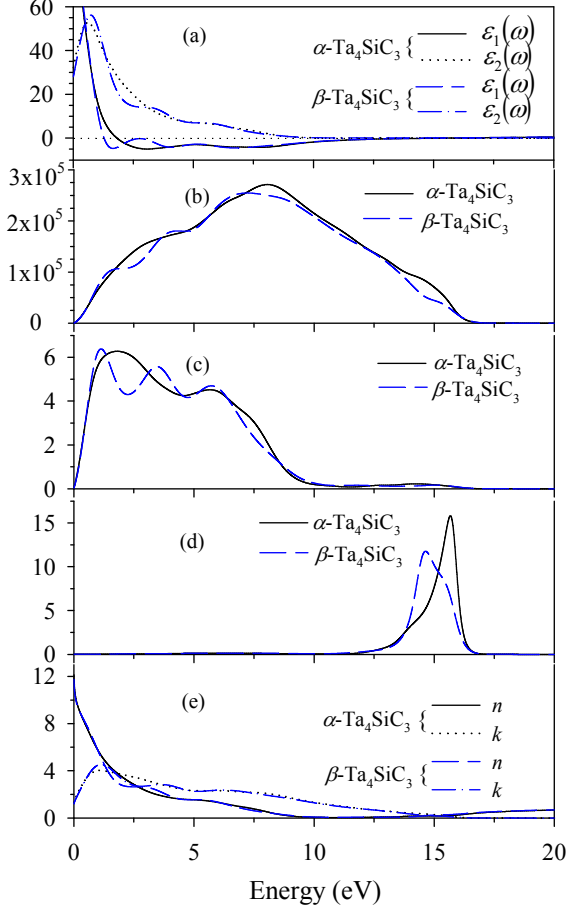


Fig. 4. Optical constants of α - and β -Ta₄SiC₃: (a) Imaginary part $\epsilon_2(\omega)$ and real part $\epsilon_1(\omega)$ of the dielectric function $\epsilon(\omega)$, (b) absorption spectrum, (c) photo-conductivity, (d) energy-loss spectrum, and (e) refractive index.

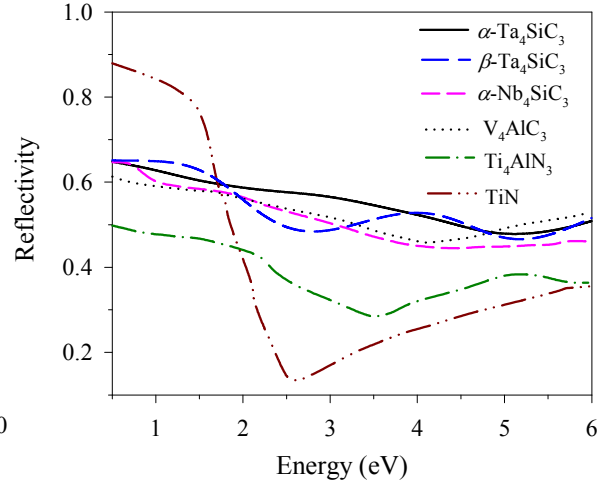


Fig. 5. Reflectivity spectra of α -Ta₄SiC₃, α -Nb₄SiC₃, V₄AlC₃, Ti₄AlN₃ and TiN.

The energy loss of a fast electron traversing in the material is manifested in the energy-loss spectrum [41]. Its peak is defined as the bulk plasma frequency ω_p , which occurs at $\epsilon_2 < 1$ and ϵ_1 reaches the zero point [42, 43]. In the energy-loss spectrum (Fig. 4d), we see that the plasma frequency ω_p for α -Ta₄SiC₃ is 15.7 eV (14.6 for β -phase). When the frequency of incident light is higher than the plasma frequency, the material becomes transparent. The real part (refractive index, n) and imaginary part (extinction coefficient, k) of the complex refractive index have been shown in Fig. 4e.

The reflectivity as a function of energy for both phases Ta₄SiC₃ is illustrated in Fig. 5. The spectra of V₄AlC₃ [37], α -Nb₄SiC₃, Ti₄AlN₃ and TiN [36] are also shown in the figure for comparison. The reflectance spectrum of α -Ta₄SiC₃ is rather flat with no strong edge and color (but β -Ta₄SiC₃ has a reflectance drop at ~ 2.77 eV). These characteristics of α -Ta₄SiC₃ are nearly similar to those of α -Nb₄SiC₃, V₄AlC₃ (see Fig. 5). On the other hand, the spectrum of TiN has sharp reflectance drop between 1.35 and 2.6 eV, which is characteristic of high conductance. TiN has high reflectivity in the infrared and low

reflectivity (transparency) for shorter wavelengths [44]. The low reflectance in the region of blue and violet light (2.8 - 3.5 eV) for TiN gives its goldlike color [45]. Therefore, the spectrum of TiN is selective. We can see that the spectrum of α -Ta₄SiC₃ is nonselective, similar to those of transition metals. According to the nonselective characteristic of the reflectance spectrum, α -Ta₄SiC₃ could reduce solar heating and enhance the infrared emittance and therefore the equilibrium temperature of its surface will be moderate in strong sunlight.

In Fig. 5, the reflectance spectra for α -Ta₄SiC₃ and α -Nb₄SiC₃ at 0.5 eV are the same but at 6.0 eV, the reflectivity of α -Ta₄SiC₃ is higher than that of α -Nb₄SiC₃. This indicates that the reflectivity of α -Ta₄SiC₃ is always higher than those of α -Nb₄SiC₃, V₄AlC₃, Ti₄AlN₃. Therefore, the capability of α -Ta₄SiC₃ to reflect solar light is stronger than α -Nb₄SiC₃, V₄AlC₃ and Ti₄AlN₃.

4. Conclusions

In conclusion, a new layered-ternary Ta₄SiC₃ compound in two phases has been predicted using first-principles calculations. The structural stability and mechanical, electronic and optical properties are then made. The elastic constants, bulk modulus, shear modulus and Young's moduli of α - and β -Ta₄SiC₃ are compared to those of other similar M₄AX₃ compounds. Both the structures are found to be stable mechanically. The results show that both the phases show ductile behavior but α - phase is found to possess higher hardness than any of the similar M₄AX₃ compounds. Further, α -Ta₄SiC₃ shows largely anisotropic elasticity but β -Ta₄SiC₃ is nearly isotropic. The electronic band structures for both the phases show metallic conductivity. Moreover, the Ta-Si bonding is weaker than the Ta-C bonding in Ta₄SiC₃ indicating that the Ta-C bond is more resistant to deformation than the Ta-Si bond. Lastly, the optical constants e.g. the reflectivity spectrum of Ta₄SiC₃ indicates that the predicted compound might be a better candidate material as a coating to avoid solar heating than the other existing α -Nb₄SiC₃, V₄AlC₃, Ti₄AlN₃ and TiN compounds. It is expected that our prediction would stimulate experimental study on the compound.

References

- [1] M. W. Barsoum, Prog. Solid State Chem. 28 (2000) 201-281.
- [2] M. W. Barsoum, H. -I. Yoo, I. K. Polushina, V. Yu. Rud, Yu. V. Rud, T. El-Raghy, Phys. Rev. B 62 (2000) 10194-10198.
- [3] J. Y. Wang, Y. C. Zhou, Phys. Rev. B 69 (2004) 144108 [13 pages].
- [4] R. Yu, X. F. Zhan, L. L. He, H. Q. Ye, J. Mater. Res. 20 (2005) 1180-1185.
- [5] A. Grechnev, S. Li, R. Ahuja, O. Eriksson, U. Jansson, O. Wilhelmsson, Appl. Phys. Lett. 85 (2004) 3071-3073.
- [6] T. El-Raghy, A. T. Procopio, C. J. Rawn, M. W. Barsoum, W. D. Porter, H. Wang, C. R. Hubbard, J. Appl. Phys. 87 (2000) 8407-8414.
- [7] B. Manoun, S. K. Saxena, Appl. Phys. Lett. 88 (2006) 201902 [3 pages].
- [8] J. P. Palmquist, T. El-Raghy, J. Höwing, O. Wilhelmsson, M. Sundberg, Abstract #ICACC-S1-184, Cocoa Beach, FL, January 2006, in: 30th International Conference on Advanced Ceramics and Composites, 2006.
- [9] Z. J. Lin, M. J. Zhuo, Y. C. Zhou, M. S. Li, J. Y. Wang, J. Mater. Res. 21 (2006) 2587.
- [10] P. Eklund, J. P. Palmquist, J. Höwing, D. H. Trinh, T. El-Raghy, H. Högberg, L. Hultman, Acta Mater. 55 (2007) 4723-4729.
- [11] Z. J. Lin, M. J. Zhuo, Y. C. Zhou, M. S. Li, J. Y. Wang, J. Amer. Ceram. Soc. 89 (2006) 3765-3769.
- [12] J. Etzkorn, M. Ade, H. Hillebrecht, Inorg. Chem. 46 (2007) 1410-1418.

- [13] C. F. Hu, Z. J. Lin, L. F. He, Y. W. Bao, J. Y. Wang, M. S. Li, Y. C. Zhou, *J. Am. Ceram. Soc.* 90 (2007) 2542-2548.
- [14] C. J. Rawn, M. W. Barsoum, T. El-Raghy, A. Prociopio, C. M. Hoffmann, C. R. Hubbard, *Mater. Res. Bull.* 35 (2000) 1785.
- [15] J. Etzkorn, M. Ade, D. Kozzot, M. Kleczek, H. Hillebrecht, *J. Solid State Chem.* 182 (2009) 995-1002.
- [16] C. F. Hu, F. Z. Li, J. Zhang, J. M. Wang, J. Y. Wang, Y. C. Zhou, *Scr. Mater.* 57 (2007) 893-896.
- [17] J. Etzkorn, M. Ade, H. Hillebrecht, *Inorg. Chem.* 46 (2007) 7646-7653.
- [18] J. P. Palmquist, S. Li, P. O. Å. Persson, J. Emmerlich, O. Wilhelmsson, H. Hogberg, M. I. Katsnelson, B. Johansson, R. Ahuja, O. Eriksson, L. Hultman, U. Jansson, *Phys. Rev. B* 70 (2004) 165401 [13 pages].
- [19] H. Högberg, P. Eklund, J. Emmerlich, J. Birch, L. Hultman, *J. Mater. Res.* 20 (2005) 779-782.
- [20] Z. Lin, M. Li, Y. Zhou *J. Mater. Sci. Technol.* 23 2 (2007) 145-165.
- [21] S. J. Clark M. D. Segall, M. J. Probert, C. J. Pickard, P. J. Hasnip, M. C. Payne, *Z. Kristallogr.* 220 (2005) 567-570.
- [22] J. P. Perdew, K. Burke, M. Ernzerhof, *Phys. Rev. Lett.* 77 (1996) 3865-3868.
- [23] D. Vanderbilt, *Phys. Rev. B* 41 (1990) 7892-7895.
- [24] H. J. Monkhorst, J. D. Pack, *Phys. Rev. B* 13 (1976) 5188-5192.
- [25] Y. L. Du, Z. M. Sun, H. Hashimoto, W. B. Tian, *Solid State Commun.* 145 (2008) 461-464.
- [26] X. H. Deng, B. B. Fan, W. Lu, *Solid State Commun.* 149 (2009) 441-444.
- [27] Z. J. Lin, M. J. Zhuo, Y. C. Zhou, M. S. Li, J. Y. Wang, *J. Mater. Res.* 22 (2007) 816-820.
- [28] R. Hill, *Proc. Phys. Soc. London A* 65 (1952) 349-354.
- [29] M. A. Hossain, A. K. M. A. Islam, F. N. Islam, *J. Sci. Res.* 1 (2) (2009) 182-191.
- [30] A. Bouhemadou, *Brazilian J. Phys.* 40 (2010) 52-57.
- [31] Q. K. Hu, Q. H. Wu, Y. M. Ma, L. J. Zhang, Z. Y. Liu, J. L. He, H. Sun, H. T. Wang, Y. J. Tian, *Phys. Rev. B* 73 (2006) 214116 [5 pages].
- [32] I. R. Shein, A. L. Ivanovskii, [arXiv.org > cond-mat > arXiv:1004.1020](https://arxiv.org/abs/cond-mat/1004.1020).
- [33] J. Y. Wang, Y. C. Zhou, T. Liao, Z. J. Lin, *Appl. Phys. Lett.* 89 (2006) 021917 [3 pages].
- [34] S. F. Pugh, *Phil. Mag.* 45 (1954) 823.
- [35] J. Haines, J. M. Leger, G. Bocquillon, *Ann. Rev. Mater. Res.* 31 (2001) 1-23.
- [36] C. Li, J. Kuo, B. Wang, Y. Li, R. Wang, *J. Phys. D: Appl. Phys.* 42 (2009) 075404 [5 pages].
- [37] C. Li, B. Wang, Y. Li, R. Wang, *J. Phys. D: Appl. Phys.* 42 (2009) 065407 [5 pages].
- [38] O. L. Anderson, *J. Phys. Chem. Solids* 24 (1963) 909-917.
- [39] P. Finkel, M. W. Barsoum, T. El-Raghy, *J. Appl. Phys.* 87 (2000) 1701 [3 pages].
- [40] J. Sun, X. F. Zhou, Y. X. Fan, J. Chen, H. T. Wang, *Phys. Rev. B* 73 (2006) 045108 [10 pages].
- [41] M. Xu, S. Y. Wang, G. Yin, J. Li, Y. X. Zheng, L. Y. Chen, Y. Jia, *Appl. Phys. Lett.* 89 (2006) 151908 [3 pages].
- [42] R. Saniz, L. H. Ye, T. Shishidou, A. J. Freeman, *Phys. Rev. B* 74 (2006) 014209 [7 pages].
- [43] J. S. De- Almeida, R. Ahuja, *Phys. Rev. B* 73 (2006) 165102 [6 pages].
- [44] M. Brogren, G. L. Harding, R. Karmhag, C. G. Ribbing, G. A. Niklasson, L. Stenmark, *Thin Solid Films* 370 (2000) 268-277.
- [45] A. Delin, O. Eriksson, R. Ahuja, B. Johansson, M. S. S. Brooks, T. Gasche, S. Auluck, J. M. Wills, *Phys. Rev. B* 54 (1996) 1673-1681.